Eur. Phys. J. A **13**, 75–79 (2002)

THE EUROPEAN PHYSICAL JOURNAL A

Quantum Monte Carlo calculations of light nuclei

Steven C. Pieper

Physics Division, Argonne National Laboratory, Argonne IL 60439, USA

Received: 1 May 2001 / Revised version: 25 August 2001

Abstract. Quantum Monte Carlo calculations using realistic two- and three-nucleon interactions are presented for nuclei with up to ten nucleons. Our Green's function Monte Carlo calculations are accurate to ∼1–2% for the binding energy. We have constructed Hamiltonians using the Argonne v_{18} NN interaction and reasonable three-nucleon interactions that reproduce the energies of these nuclear states with only ∼500 keV rms error. Other predictions, such as form factors, decay rates, and spectroscopic factors also agree well with data. Some of these results are presented to show that *ab initio* calculations of light nuclei are now well in hand.

PACS. 21.10.-k Properties of nuclei; nuclear energy levels – 21.45.+v Few-body systems – 21.60.Ka Monte Carlo models – 27.20.+n $6 \leq A \leq 19$

1 Introduction

A major goal in nuclear physics is to understand how nuclear binding, stability, and structure arise from the underlying interactions between individual nucleons. To achieve this goal, we must both determine the Hamiltonian to be used, and devise reliable methods for many-body calculations using it. In principle, quantum chromodynamics can prescribe the nuclear Hamiltonian, but it will be a long time before this will be done with useful accuracy. Thus, the nuclear Hamiltonian is determined phenomenologically, and our knowledge of it is refined, in part, by the many-body calculations we make with it. The Hamiltonian has both two- and three-nucleon terms with strong spin, tensor, and isospin dependence.

Exact (defined here to mean an error of less than 1% in the computed binding energy) many-body calculations with such a Hamiltonian are very complicated, and it is only in the last five years that results have been obtained for $A \geq 6$; these are discussed in this contribution. The methods and results presented here are from the work of the Argonne, Los Alamos, TJNAF, and Urbana groups; complete descriptions of our VMC and GFMC calculations may be found in refs. [1] and [2].

2 The nuclear Hamiltonian

Our Hamiltonian includes a non-relativistic one-body kinetic energy, the Argonne v_{18} two-nucleon potential [3] and various three-nucleon potentials,

$$H = \sum_i \left(-\frac{\hbar^2}{2m} \nabla_i^2 \right) + \sum_{i<j} v_{ij} + \sum_{i<j<k} V_{ijk} \ . \qquad (1)$$

The difference between proton and neutron masses is included in our calculations, but ignored above. The Argonne v_{18} potential is one of a number of new, highly accurate NN potential models developed since 1990. It can be written as a sum of electromagnetic and one-pion–exchange terms and a shorter-range phenomenological part. The electromagnetic terms include one- and two-photon–exchange Coulomb interactions, vacuum polarization, Darwin-Foldy, and magnetic moment terms, with appropriate proton and neutron form factors.

The one-pion–exchange part contains the normal Yukawa and tensor functions with a short-range cutoff. This and the remaining phenomenological part of the potential can be written as a sum of eighteen operators, which is where the name v_{18} comes from. The first fourteen are charge independent, and include spin-spin, tensor, $L \cdot S$, and quadratic-L terms, each with a dependence on isospin. The last four operators break charge independence. The radial forms associated with each operator are determined by fitting NN scattering data. The potential was fit directly to the Nijmegen NN scattering data base [4], which contains 1787 pp and 2514 np data in the range 0–350 MeV, with a χ^2 per datum of 1.09. It was also fit to the nn scattering length measured in $d(\pi^-, \gamma)nn$ experiments and the deuteron binding energy.

For many years, we have used the Urbana series of three-nucleon potentials; the current (ninth) model is designated UIX. These potentials are written as sums of two-pion–exchange (with intermediate excitation of an isobar) and shorter-range phenomenological terms. The two-pion–exchange term, $V_{ijk}^{2\pi,P}$, is that of the original Fujita-Miyazawa model [5] and contains both spin (tensor) and isospin dependence. The shorter-range phenomenological

term, V_{ijk}^R, is purely central and repulsive. Our recent work has shown the need for additional overall V_{ijk} binding for p shell nuclei and for further increased binding as $|N-Z|$ increases. This has led to the development of "Illinois" models [6] which, in addition to the Urbana terms, contain the two-pion S-wave scattering term, $V_{ijk}^{2\pi,S}$, and three-pion–exchange ring terms, $V_{ijk}^{3\pi}$. The latter can involve the excitation of one or two sequential isobars, so that the energy denominators contain only one Δ mass.

In light nuclei we find that the three-nucleon potential contributes only 2–9% (increasing with A) of the total potential energy. However, due to the large cancellation of potential and kinetic energy, this amounts to 15–50% (increasing mostly with $N-Z$) of the binding energy. We expect a similar ratio for the four-body potential, which implies that it contributes only a few percent of the binding energy, with the largest contributions in the nuclei that are least accurately computed.

3 Quantum Monte Carlo

Variational Monte Carlo finds an upper bound, $E_{\rm T}$, to an eigen energy of H by evaluating the expectation value of H in a trial wave function, $\Psi_{\rm T}$. The parameters in $\Psi_{\rm T}$ are varied to minimize $E_{\rm T}$, and the lowest value is taken as the approximate energy. Over the years, we have developed rather sophisticated $\Psi_{\rm T}$ for light nuclei [1,2]. These contain symmetrized products over all pairs of (non-commuting) two-body operators (the most important being the tensor-isospin correlation corresponding to the pion-exchange potential) and sums of non-central three-body correlations induced by V_{ijk}. These act on an antisymmetric one-body piece which determines the quantum numbers of the state being computed. The one-body piece is constructed using coordinates relative to the c.m. (or to a sub-cluster c.m.), and the two- and three-body correlations all use differences of positions, so the entire wave function is translationally invariant. The products of two-body operators are symmetrized so the entire wave function is antisymmetric.

GFMC projects out the lowest-energy ground state from the VMC $\Psi_{\rm T}$ by using

$$\Psi(\tau) = e^{-(H-E_0)\tau}\Psi_{\rm T}\ ; \tag{2}$$

$$\Psi_0 = \lim_{\tau\to\infty}\Psi(\tau). \tag{3}$$

If sufficiently large τ is reached, the eigenvalue E_0 is calculated exactly while other expectation values are generally calculated neglecting terms of order $|\Psi_0-\Psi_{\rm T}|^2$ and higher. In contrast, the error in the variational energy, $E_{\rm T}$, is of order $|\Psi_0-\Psi_{\rm T}|^2$, and other expectation values calculated with $\Psi_{\rm T}$ have errors of order $|\Psi_0-\Psi_{\rm T}|$.

Here I present a simplified overview of nuclear GFMC; a rather complete discussion may be found in [1,2]. Introducing a small time step, $\triangle\tau$, $\tau = n\triangle\tau$, gives (typically $\triangle\tau = 0.5\ \mathrm{GeV}^{-1}$)

$$\Psi(\tau) = \left[e^{-(H-E_0)\triangle\tau}\right]^n \Psi_{\rm T} = G^n\Psi_{\rm T}\,, \tag{4}$$

where G is the short-time Green's function. The $\Psi(\tau)$ is represented by a vector function of $\mathbf{R}$, and the Green's function, $G_{\alpha\beta}(\mathbf{R}',\mathbf{R})$ is a matrix function of $\mathbf{R}'$ and $\mathbf{R}$ in spin-isospin space (labeled by the subscripts α,β), defined as

$$G_{\alpha\beta}(\mathbf{R}',\mathbf{R}) = \langle \mathbf{R}',\alpha|e^{-(H-E_0)\triangle\tau}|\mathbf{R},\beta\rangle. \tag{5}$$

Omitting spin-isospin indices for brevity, the GFMC wave function after n time steps at a specific point, $\mathbf{R}_n$, is given by

$$\Psi(\mathbf{R}_n,\tau) = \int G(\mathbf{R}_n,\mathbf{R}_{n-1})\cdots G(\mathbf{R}_1,\mathbf{R}_0)\Psi_{\rm T}(\mathbf{R}_0) \,\mathrm{d}\mathbf{R}_{n-1}\cdots\mathrm{d}\mathbf{R}_1\mathrm{d}\mathbf{R}_0, \tag{6}$$

and the integration is done by Monte Carlo. We approximate the short-time propagator as a symmetrized product of exact two-body propagators, $g_{ij}(\mathbf{r}_{ij},\mathbf{r}'_{ij})$, and include the V_{ijk} to first order:

$$\begin{aligned} G_{\alpha\beta}(\mathbf{R},\mathbf{R}') = {} & e^{E_0\triangle\tau}G_0(\mathbf{R},\mathbf{R}') \\ & \times\exp\left[-\frac{\triangle\tau}{2}\sum(V_{ijk}^R(\mathbf{R})+V_{ijk}^R(\mathbf{R}'))\right] \\ & \times\langle\alpha|I_3(\mathbf{R})|\gamma\rangle\langle\gamma|\left[\mathcal{S}\prod_{i<j}\frac{g_{ij}(\mathbf{r}_{ij},\mathbf{r}'_{ij})}{g_{0,ij}(\mathbf{r}_{ij},\mathbf{r}'_{ij})}\right]|\delta\rangle \\ & \times\langle\delta|I_3(\mathbf{R}')|\beta\rangle\ , \end{aligned} \tag{7}$$

where G_0 is the free many-body propagator and $g_{0,ij}$ is the free two-body propagator.

The construction of the exact two-body propagator is described in ref. [1]. The influence of the three-nucleon potential on the many-body propagator is broken into two pieces: the scalar V_{ijk}^R which is easily exponentiated, and the 2- and 3-pion terms which are complicated operators in spin-isospin space. The simplest treatment of these terms is to expand to first order in $\triangle\tau$,

$$I_3(\mathbf{R}) = 1 - \frac{\triangle\tau}{2}\sum V_{ijk}^\pi(\mathbf{R})\,, \tag{8}$$

where V_{ijk}^π designates all the non-central terms in V_{ijk}. In fact, parts of the V_{ijk}^π can be included in the symmetrized products of two-body propagators.

For more than four nucleons, GFMC calculations suffer significantly from the well-known fermion sign problem. This arises from the fact that the stochastic application of the propagator, $G_{\alpha\beta}$, does not preserve the antisymmetry of $\Psi_{\rm T}$. The resulting symmetric admixture has a lower energy and thus grows exponentially in amplitude. Expectation values with $\Psi_{\rm T}$ stochastically discard the symmetric components, thus they make a contribution to the statistical errors. The resulting exponential growth of the statistical errors as one propagates to larger τ, or as A is increased, effectively limits unconstrained GFMC p shell calculations to $\tau \le 0.06\ \mathrm{MeV}^{-1}$. This means that any errors in $\Psi_{\rm T}$ corresponding to excitations of less than ~ 20 MeV will be damped out by less than $1/e$. In practice, we find that the dependence of the GFMC energy

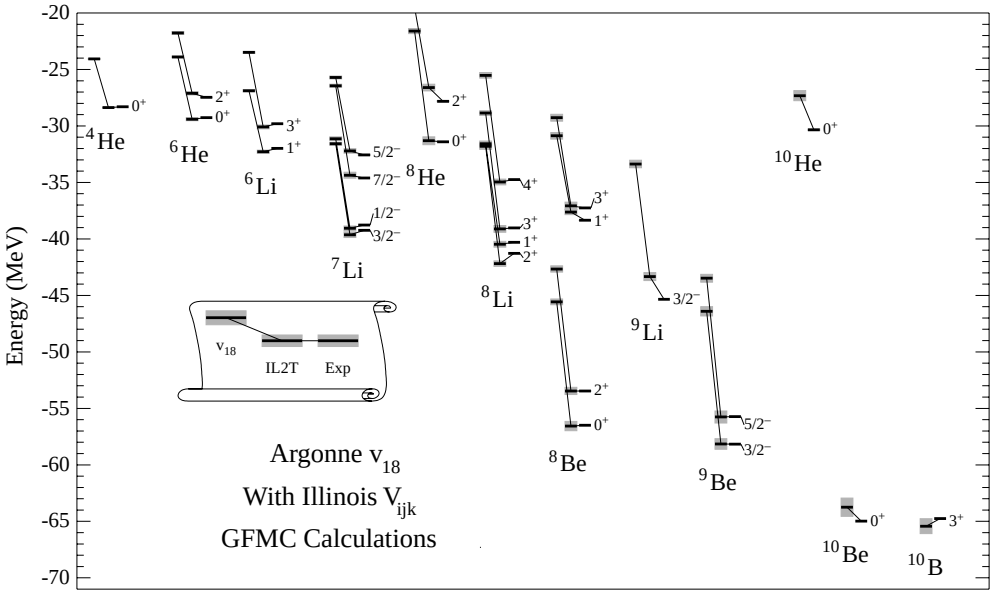

Fig. 1. Computed and experimental levels of light nuclei; Illinois potential results are preliminary.

on τ corresponds to the removal of small admixtures of states with very high energies ($\sim$ 0.1 to 2 GeV), and so most of the errors in the $\Psi_{\rm T}$ are completely removed by $\tau = 0.06$ MeV^{-1}. However reliable calculations for $A \geq 8$ require a solution to the fermion sign problem.

In the last two years we have developed and extensively tested a constrained-path algorithm for nuclear GFMC [2]. In this method configurations with small or negative $\Psi(\tau)^\dagger \cdot \Psi_{\rm T}$ are discarded such that the average over all discarded configurations of $\Psi(\tau)^\dagger \cdot \Psi_{\rm T}$ is 0. This means that, if $\Psi_{\rm T}$ were the true eigenstate, the discarded configurations would contribute nothing but noise to $\langle H \rangle$. This constrained propagation completely controls the growth of the statistical errors and in most cases produces a result that is statistically the same as unconstrained propagation (the accuracy of the comparison may be limited by the statistical errors in the unconstrained result). However, we have demonstrated some cases for which constrained propagation leads to a wrong result, and in fact for which the approximate $\langle H \rangle$ is not even an upper bound to the correct eigenvalue. In all cases the correct result can be obtained by making a few (10–20) unconstrained steps before evaluating the energy.

The number of spin-isospin components in $\Psi_{\rm T}$ grows rapidly with the number of nucleons. Thus a calculation of a state in ^{8}Be involves about 30 times more floating-point operations than one for ^{6}Li, and ^{10}Be requires 50 times more than ^{8}Be. Calculations of the sort being described here are currently feasible up to only $A = 10$; these require $\sim$15000 cpu hours on the NERSC IBM SP running at 140 MFLOPS/cpu (7.5×10^{15} operations). We expect to extend these to ^{12}C in the next few years, but other methods are needed for larger nuclei.

Comparison of the VMC and GFMC energies shows that the variational wave functions for the s-shell nuclei are quite accurate — the GFMC improves the VMC energy of ^{4}He by only 0.56 MeV (2%). However, the p-shell variational wave functions are much less accurate; compared to the GFMC energies for the same Hamiltonian, they result in under bindings of 3.3 MeV (10%) for ^{6}Li to 8 MeV (16–35%) for the 8-body nuclei. On the other hand, the excitation spectra from VMC and GFMC calculations are quite similar.

4 Some results

Only a few of our results can be presented here; many other results may be found in [1,2,7–10]; results with the new Illinois potentials are being prepared for publication. Figure 1 compares GFMC energies computed using just the Argonne v_{18}, and using v_{18} plus one of the new Illinois V_{ijk} (provisionally called IL2T) with experiment. The Illinois V_{ijk} are still preliminary. Only statistical errors are shown for the Monte Carlo calculations; we believe that the GFMC calculations are converged to $\sim$ 0.3 MeV for $A = 6$ and $\sim$ 0.6 MeV for $A = 10$, but studies of the $A = 10$ calculations are still in progress. The difference between the two models shows the importance of the V_{ijk}. This Illinois potential, and several others, does a very good job of reproducing the nuclear levels in this region; the rms error in the computed energies is 600 keV for 22 experimentally narrow levels with $A \leq 10$. For the 17 narrow levels with $A \leq 8$, the rms error is only 320 keV. In contrast, the same 17 levels result in a 7.7 MeV rms error if no V_{ijk} is used and a 2.3 MeV rms error with the older Urbana IX V_{ijk}.

The important improvement in the Illinois potentials is the addition of three-pion ring terms ($V_{ijk}^{3\pi}$). These are repulsive in $T = \frac{1}{2}$ triples and attractive in $T = \frac{3}{2}$ triples and thus can correct the deficiencies of the Urbana models, which were developed for calculations of s-shell nuclei that

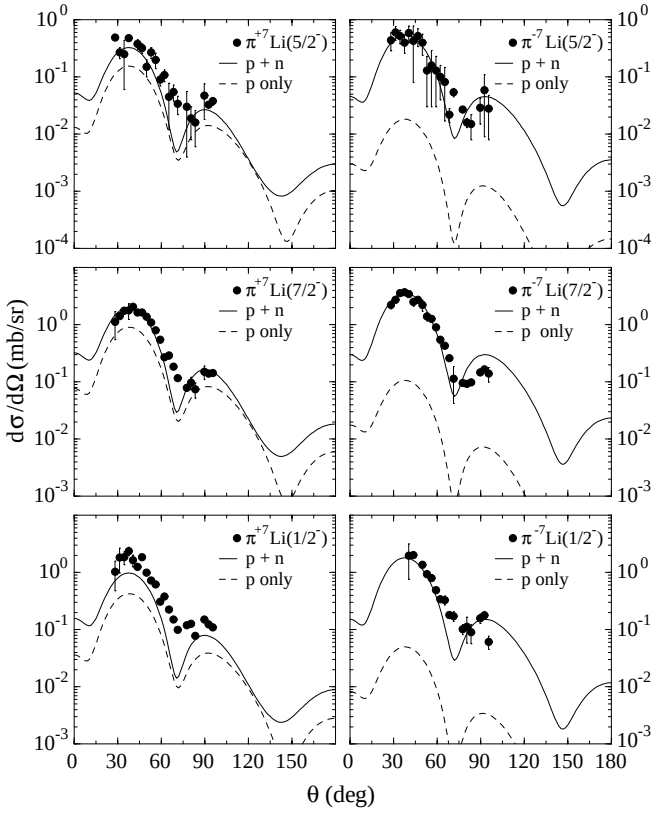

Fig. 2. Inelastic pion scattering from ^{7}Li at 164 MeV.

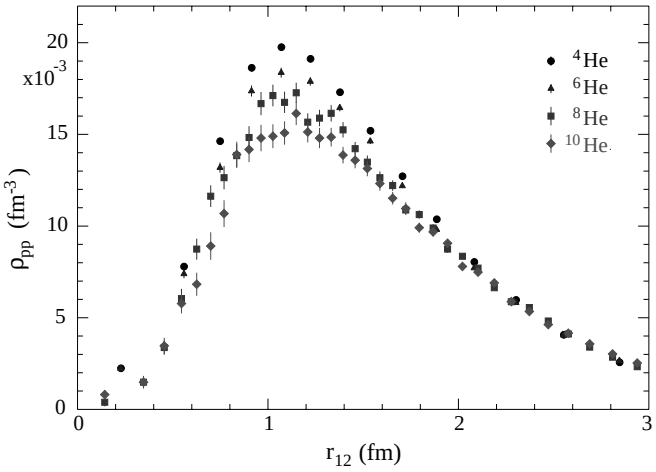

Fig. 3. Computed pp distributions in helium isotopes.

have no $T = \frac{3}{2}$ triples. The $V_{ijk}^{2\pi,S}$ turns out to be small and nearly proportional to the $V_{ijk}^{2\pi,P}$ in the Urbana models; thus it does not provide any new ability to fit the nuclear energies.

We have used our VMC wave functions to compute other experimental properties of these nuclei and will be extending these calculations to the GFMC wave functions in the next year. Some examples are:

- Both elastic and inelastic electron-scattering form factors for ^{6}Li [7]. Our results agree very well with the data without the need for effective nucleon charges.
- Quasihole wave functions for $p + {}^6$He in ^{7}Li [8]. These were used to predict $^7\mathrm{Li}(e, e'p)$ to the ground and excited states of ^{6}He, including the absolute spectroscopic factor, in perfect agreement with the data.
- Isovector and isotensor energy coefficients for mirror nuclei (Nolen-Schiffer anomaly) [2]. In this case the GFMC calculations have already been done and are generally in good agreement with the data.
- Isospin-mixing matrix elements for states of ^{8}Be which are in much better agreement with the data than previous calculations [2].
- Low-energy reaction rates for astrophysically interesting processes. The $^4\mathrm{He}(d,\gamma)^6\mathrm{Li}$, reaction is the subject of recent work by Nollett, Wiringa, and Schiavilla [9].

A recent example of these studies is the calculation by Lee and Wiringa of $^{6,7}\mathrm{Li}(\pi,\pi')$ reactions [10]. The data was taken more than 20 years ago [11] and originally analyzed using shell-model wave functions by Lee and Kurath [12]. This analysis could reproduce the magnitudes of the cross-sections by using large, but standard, renormalizations of 2.5 for π-proton scattering and 1.75 for π-neutron scattering. The modern analysis uses our VMC wave functions which have strong short- and intermediate-ranged correlations induced by the NN potentials. In a shell-model picture, which we do not use, these correlations result in the wave functions having substantial components of very high $\hbar\omega$. Using these wave functions for the various states of ^{7}Li and the same optical-model scattering states as were used by Lee and Kurath, the absolute normalizations of the the data are directly predicted, as is shown in fig. 2. This is particularly gratifying for the π^- scattering which, as is shown in the right-hand panels of the figure, is dominated by scattering from neutrons. The proton distributions of our wave functions had already been well tested by comparisons with $(e, e'p)$ scattering [7], but this is the first direct test of the neutron distributions predicted by the wave functions.

An interesting question is how inert is the alpha-particle core in larger nuclei. At present, this cannot be directly determined experimentally but some light can be cast on it by our GFMC calculations of isotopes of helium. The proton density distribution of the alpha-particle peaks at a value comparable to nuclear-matter density; that is, since the neutron and proton densities of ^{4}He are almost identical, the near-central density of ^{4}He is nearly twice that of equilibrium nuclear matter. In heavier helium isotopes, the center of mass of the alpha core is pushed around and the proton density is much less peaked. Because this is a result of just moving the alpha around, it says nothing about possible changes in the alpha's structure in these isotopes. However, the proton-proton pair distribution, ρ_{pp} is independent of center-of-mass motion. Also in helium isotopes the single pp pair is in the alpha core. Thus, any change in ρ_{pp} as one adds neutrons to ^{4}He does indicate a change in the internal structure of the alpha core.

Figure 3 shows the ρ_{pp} for ^{4,6,8,10}He from our GFMC calculations. The normalization of each of the distributions is 1.0, so the reduction in the peak height as more neutrons are added is necessarily compensated by small increases in the tails of the distributions. We see that there is a small, but statistically significant, polarization of the alpha by the surrounding neutrons. This is presumably arising from two effects: an actual pulling apart of the alpha by the neutrons, and charge-exchange correlations with the surrounding neutrons. Due to the total antisymmetry of our wave functions, we cannot distinguish between these two possibilities.

The last few years have seen much progress in nuclear QMC calculations. The energy predictions of a given realistic Hamiltonian can be found with 1–2% accuracy for up to ten nucleons and Hamiltonians can be constructed that reproduce the light nuclei with this accuracy.

This work is supported, in part, by the U. S. Department of Energy, Nuclear Physics Division, under contract No. W-31-109-ENG-38. The calculations were made possible by generous grants of time on the parallel computers of the Mathematics and Computer Science Division, Argonne National Laboratory, and on the IBM SP at the National Energy Research Scientific Computing Center.

References

1. B.S. Pudliner, V.R. Pandharipande, J. Carlson, S.C. Pieper, R.B. Wiringa, Phys. Rev. C **56**, 1720 (1997).
2. R.B. Wiringa, S.C. Pieper, J. Carlson, V.R. Pandharipande, Phys. Rev. C **62**, 014001 (2000).
3. R.B. Wiringa, V.G.J. Stoks, R. Schiavilla, Phys. Rev. C **51**, 38 (1995).
4. J.R. Bergervoet *et al.*, Phys. Rev. C **41**, 1435 (1990); V.G.J. Stoks, R.A.M. Klomp, M.C.M. Rentmeester, J.J. de Swart, Phys. Rev. C **48**, 792 (1993).
5. J. Fujita, H. Miyazawa, Prog. Theor. Phys. **17**, 360 (1957).
6. S.C. Pieper, V.R. Pandharipande, J. Carlson, R.B. Wiringa, Phys. Rev. C **64**, 014001 (2001).
7. R.B. Wiringa, R. Schiavilla, Phys. Rev. Lett. **81**, 4317 (1998).
8. L. Lapikás, J. Wesseling, R.B. Wiringa, Phys. Rev. Lett. **82**, 4404 (1999).
9. K.M. Nollett, R.B. Wiringa, R. Schiavilla, Phys. Rev. C **63**, 024003 (2001) nucl-th/0006064.
10. T.-S.H. Lee, R.B. Wiringa, Phys. Rev. C **63**, 014006 (2000).
11. J. Bolger, E. Boshitz, R. Mischke, A. Nagel, W. Saathoff, C. Wiedner, J. Zichy, in *Meson-Nuclear Physics 1979, Proceedings of the 2nd International Conference, Houston, Texas*, edited by E.V. Hungerford III, AIP Conf. Proc. Vol. **54** (AIP, New York, 1979) p. 519.
12. T.-S.H. Lee, D. Kurath, Phys. Rev. C **21**, 293 (1980); **22**, 1670 (1980).